Tonotopic Gradients of Eph Family Proteins in the Chick Nucleus Laminaris during Synaptogenesis

Abigail L. Person,[1] Douglas Pat Cerretti,[2] Elena B. Pasquale,[3] Edwin W. Rubel,[4,5] Karina S. Cramer[5]*

[1] Neurobiology and Behavior Program, University of Washington, Seattle, Washington 98195

[2] Department of Vascular Biology, Amgen Corporation, Seattle, Washington 98101

[3] Neurobiology Program, Burnham Institute, La Jolla, California 92037

[4] Department of Physiology and Biophysics, University of Washington, Seattle, Washington 98195

[5] Virginia Merrill Bloedel Hearing Research Center, Department of Otolaryngology, Head and Neck Surgery, University of Washington, Seattle, Washington 98195

Received 6 June 2003; accepted 8 September 2003

ABSTRACT: **Topographically precise projections are established early in neural development. One such topographically organized network is the auditory brainstem. In the chick, the auditory nerve transmits auditory information from the cochlea to nucleus magnocellularis (NM). NM in turn innervates nucleus laminaris (NL) bilaterally. These projections preserve the tonotopy established at the level of the cochlea. We have begun to examine the expression of Eph family proteins during the formation of these connections. Optical density measurements were used to describe gradients of Eph proteins along the tonotopic axis of NL in the neuropil, the somata, and the NM axons innervating NL at embryonic day 10, when synaptic connections from NM to NL are established. At E10–11, NL dorsal neuropil expresses EphA4 at a higher concentration in regions encoding high frequency sounds, decreasing in concentration monotonically toward the low frequency (caudolateral) end. In the somata, both EphA4 and ephrin-B2 are concentrated at the high frequency end of the nucleus. These tonotopic gradients disappear between E13 and E15, and expression of these molecules is completely downregulated by hatching. The E10–11 patterns run counter to an apparent gradient in dendrite density, as indicated by microtubule associated protein 2 (MAP2) immunolabeling. Finally, ephrin-B2 is also expressed in a gradient in tissue ventral to the NL neuropil. Our findings thus suggest a possible conserved mechanism for establishing topographic projections in diverse sensory systems. These results of this study provide a basis for the functional examination of the role of Eph proteins in the formation of tonotopic maps in the brainstem.** © 2004 Wiley Periodicals, Inc. J Neurobiol 60: 28–39, 2004

Keywords: **Eph receptor; ephrin; tonotopy; topography; nucleus laminaris; gradient**

INTRODUCTION

The avian auditory brainstem is a well-characterized neural circuit that has several advantageous characteristics for exploring the mechanisms of neural development and information processing. Auditory responses are conveyed into the ipsilateral brainstem nucleus magnocellularis (NM), which in turn projects to nucleus laminaris (NL) bilaterally (Rubel and Parks, 1988). Convergent inputs onto NL neuropil are thought to underlie neural calculation of interaural time differences (ITDs), which are critical for sound localization (Parks and Rubel, 1975; Young and Rubel, 1983; Carr and Konishi, 1990). In addition to the precise spatial segregation of NM inputs to NL with respect to ITD, NL afferents also maintain a topographic arrangement similar to the organization of other sensory systems. Tonotopy is established at the level of the cochlea and is present at each level of auditory processing. The axis of tonotopy extends from rostromedial (high frequency) to caudolateral (low frequency) NM and NL. This tonotopic axis has

**Present address:* Department of Neurobiology and Behavior, University of California, Irvine, 2205 McGaugh Hall, Irvine, CA 92697-4550.

Correspondence to: K. S. Cramer (cramerk@uci.edu).

Contract grant sponsor: NIDCD; contract grant number: DC00395.
Contract grant sponsor: NIDCD; contract grant number: DC04661.
Contract grant sponsor: NIDCD; contract grant number: DC05771.

DOI 10.1002/neu.10330

been quantitatively described in the mature system as well as in embryos (Rubel and Parks, 1975; Lippe and Rubel, 1985) and thereby offers an elegant preparation in which to study developmental mechanisms involved with establishing topographic projections.

While patterned spontaneous neural activity has been suggested to be important for normal development of some sensory system maps (Cline et al., 1987), this mechanism does not appear to have a dominant role in the development of topographic maps in the auditory brainstem and midbrain (Young and Rubel, 1986; Leake et al., 2002; Rubel and Cramer, 2002). In contrast, molecular guidance cues have proven crucial in the establishment of topographic projections. The Eph family of proteins, including Eph receptor tyrosine kinases and their associated membrane-bound ligands, the ephrins (Eph Nomenclature Committee, 1997), are known to directly influence the development of topographic, layer-specific projections of retinal ganglion cells to their thalamic and tectal targets in both avian and mammalian visual systems (Cheng et al., 1995; Drescher et al., 1995; Braisted et al., 1997; Connor et al., 1998; Feldheim et al., 1998; Frisén et al., 1998; Hindges et al., 2002). In addition, gradients of Eph and ephrin signaling have been shown to be involved in development of topographic organization in motor systems and other central nervous system (CNS) pathways (Gao et al., 1996; Dearborn et al., 2002). Recently, Ephs and ephrins have been shown to be expressed asymmetrically in the dorsal and ventral neuropil of NL at embryonic day (E) 9 and 10, when NM axons are first forming synapses onto NL. EphA4 expression is then symmetrical for several days before being dramatically downregulated by E18 (Cramer et al., 2000). In the present study, we characterized the expression of two Eph family proteins along the tonotopic axis of NL using immunohistochemistry. Here we report a robust tonotopic gradient of EphA4 in the dorsal neuropil of NL and ephrin-B2 in the NL somata and ventral glia surrounding NL at a developmental time point when NM axons are forming synapses on NL neuropil.

MATERIALS AND METHODS

Tissue Preparation

For the observations presented here, a total of 35 chicken embryos were collected and staged according to the Hamburger-Hamilton guide (Hamburger and Hamilton, 1951). Brainstems were dissected from embryonic day (E) 10, 11, 12, 14, 15, and 18 chicks and fixed by immersion in 4% paraformaldehyde or a solution containing 49% ethanol, 20% formalin, and 10% glacial acetic acid in dH_2O. For cryostat sections, tissue was rinsed in phosphate buffered saline (PBS) following fixation, then cryoprotected in 30% sucrose overnight at 4°C. Prior to sectioning, we made a sagittal cut along the midline and immersed the tissue in OCT medium.

For analyses of immunolabeling gradients (see below), an important aspect of this study is that tissue sections were cut parallel to the tonotopic axis of NL. The tissue was then oriented approximately 30° to the sagittal plane such that individual sections through the middle of NL would include the rostromedial to caudolateral extent of the nucleus, which is the orientation of the tonotopic axis (Rubel and Parks, 1975). Serial 10 μm sections were collected on chrome alum subbed slides and stored at −20°C. For paraffin sections, tissue was dehydrated in increasing concentrations of ethanol following fixation. Tissue was then cleared with Hemo-De (Fisher Scientific, Pittsburgh, PA) and immersed in three changes of paraffin prior to embedding in paraffin molds. Again, careful attention was paid to orientation and 10 μm sections were made 30° to the parasagittal plane, containing rostromedial to caudolateral extents of the NL. Just prior to staining, slides were immersed in xylene to remove paraffin and then rehydrated in a descending series of ethanol washes.

Immunohistochemistry

The sections from each brain were divided into five alternate section series. In all cases, one set of sections was stained for Nissl bodies with thionin. The other sections were processed for immunohistochemistry with antibodies to EphA4 ($n = 7$), ephrin-B2 ($n = 4$), or microtubule associated protein 2 (MAP2) ($n = 5$).

In order to determine the extent of dendritic label of Eph proteins, we stained E10–11 and E14–15 tissue for MAP2, which labels neuronal somata and dendrites specifically. This staining was used to define the spatial extent and density of dendritic fields for quantitative densitometric analysis (see below). The antibody against EphA4 was used in E10–11, E14–15, and E18 tissue. We stained only E10–11 tissue for ephrin-B2.

The antibodies against EphA4 and ephrin-B2 used in this study have been purified and shown to bind specifically in immunoblot assays. The EphA4 antibody is a rabbit polyclonal antibody directed against the carboxy terminus of the EphA4 receptor. It was affinity-purified and shown to be specific for EphA4 in chick tissue (Soans et al., 1994). The ephrin-B2 protein contains a spacer peptide region with a unique amino acid sequence (GSSTDBNSAGHSGNNI) against which the antibody used in this study was made. The antigen used to produce the ephrin-B2 rabbit polyclonal antibody was conjugated to ovalbumin. Thus, in order to prevent nonspecific label in chick tissue, we purified the polyclonal antibody by adsorbing anti-ovalbumin antibodies in a cyanogen bromide Sepharose column with ovalbumin conjugate (Sigma, St. Louis, MO). This process rendered

the antibody specific to ephrin-B2 in chick tissue, which was verified by Western blotting (Cramer et al., 2002).

At least three brains were processed for each antibody at E10–11 or E14–15. For cryostat sections, slides were removed from −20°C storage, allowed to reach room temperature, then rinsed in PBS to remove residual OCT. Paraffin-embedded tissue was rehydrated for immunohistochemistry by immersing slides in xylene followed by decreasing concentrations of ethanol. Finally, slides were rinsed in PBS. Subsequent steps of the immunoreactions were identical for both cryostat and paraffin-embedded tissue.

A PAP pen (The Binding Site Inc., San Diego, CA) was used to make hydrophobic wells around each section on a slide. Tissue was placed in 0.3% H_2O_2 in absolute methanol for 10 min to quench endogenous peroxidase. After rinsing in PBS, tissue was incubated in a blocking solution of 5% nonfat dry milk and 0.1% triton X-100 in PBS for 1 h.

Tissue was incubated in 1 μg/mL primary antibody in blocking solution in a humid chamber overnight at 4°C, then rinsed and incubated in 1:200 biotinylated goat anti-rabbit IgG (Vector Laboratories, Burlingame, CA) in blocking solution for 1–2 h. After extensive washing, tissue was then incubated in a solution containing an avidin horseradish peroxidase (HRP) complex (ABC, Vector) for 1 h. HRP was visualized using either the VIP substrate kit (Vector) or 0.05% diaminobenzadine. Slides were rinsed and briefly dehydrated in increasing concentrations of ethanol, then xylene, and coverslipped with DPX mounting medium (BDH Laboratory Supplies, Poole, U.K.). Alternate sections were stained for Nissl using standard thionin protocols. Negative controls were run that lacked either primary or secondary antibodies. In all cases, negative controls completely lacked staining.

Densitometry and Regression Analysis

From each brain, the section containing the longest extent of NL was chosen for quantitative analysis and imaging. Sections were photographed on a Nikon Optiphot-2 microscope using a Spot IIe digital camera and acquisition software (Diagnostic Instruments, Inc., Sterling Heights, MI). Flat-field correction was used to compensate for any unevenness in the illumination of the field.

Optical density (OD) of somata, dorsal neuropil, and ventral neuropil of NL were individually measured using Object Image software (National Institutes of Health, Bethesda, MD). In order to quantify immunolabeling in NL, we divided 40× monochrome images of NL into compartments that spanned the tonotopic axis. This process amounted to outlining short regions of the neuropil or somata of the digital image using the imaging software. For example, for a single position along the nucleus, three compartments were constructed: one outlining individual somata or groups of two to three contiguous somata, another outlining adjacent dorsal neuropil, and the third outlining adjacent ventral neuropil. The OD in each compartment outlined was then calculated. This process was performed along the length of the nucleus and yielded OD values for somata, dorsal neuropil, and ventral neuropil separately for the entire length of the nucleus.

Individual OD values were then normalized to the mean OD for each group of measurements in each animal. The mean OD was determined by averaging all measurements from a given region of NL in a single section. For example, measurements OD in dorsal neuropil for EphA4 were normalized to the mean of OD in dorsal neuropil for that animal. These data were then plotted against the tonotopic position along the nucleus, which is expressed as a fraction of the total length with the high frequency end = 0 and the low frequency end = 1. Statview software (version 5.0; SAS Institute, Inc., Cary, NC) was used to calculate correlations and linear regressions and generate the plots of OD vs. tonotopic position.

In addition to the regression analyses on these sections, normalized OD values at the HF quarter were pooled and compared to pooled OD values at the low frequency end using two-tailed paired Student's t tests.

Comparison of Immunolabeling at High vs. Low Frequency Zones

The analyses described above are most suitable when applied to the greatest extent of the tonotopic axis, which is contained in the sections having the longest extent of NL. In order to be assured of the reliability of the gradients observed in the regression analyses, we undertook an additional analysis. In E11 tissue immunolabeled for EphA4, we measured normalized OD in all labeled sections containing NL. We computed the average OD across sections for the high frequency 30% of the nucleus and the low frequency 30%. We then compared high vs. low frequency labeling for this group using a paired t test in which each animal contributed one data point.

Preparation of Photomicrographs

The nuclei used for densitometric analysis were photographed with a SpotIIe digital camera through a 25× objective and were imported into Adobe Photoshop 5.0 (Adobe Systems, Inc., San Jose, CA). The images were then cropped and adjusted for brightness and contrast, and annotated with scale bars and arrows.

RESULTS

The orientation of the tonotopic axis in NM and NL is highly stereotyped in postnatal and embryonic chicks (Rubel and Parks, 1975; Lippe and Rubel, 1985). Thus, physiological measurements of best frequency were not necessary. Sections through the brainstems of postnatal and embryonic chickens were processed for immunohistochemistry to examine the expression of EphA4, ephrin-B2, and MAP2 using antibodies that have previously

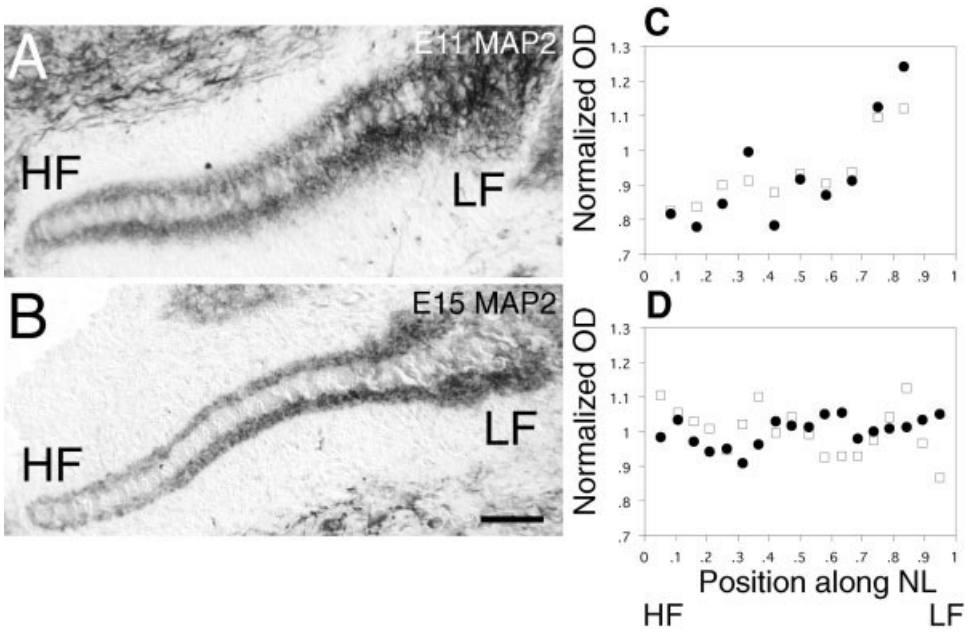

Figure 1 (A,B) Microtubule associated protein 2 (MAP2) immunolabeling in dendrites along the tonotopic axis of nucleus laminaris (NL) in paraffin sections. (A) Parasagittal section from E11 chick embryo. MAP2 is expressed in dorsal and ventral neuropil of NL, while the line of cell bodies in NL lacks expression. High frequency (HF) and low frequency (LF) regions are indicated. (B) MAP2 expression in E15 chick embryo along the tonotopic axis of NL. Both dorsal and ventral regions are immunolabeled. Note broadening of labeled region in the low frequency end of NL in both (A) and (B); this expansion corresponds with larger dendritic arbors in this region. Scale bar, 50 μm. (C,D) Densitometric analysis of MAP2 staining at E12 and E15. The abscissa represents the position along the length of NL from HF to LF. The ordinate displays optical density (OD) normalized to the mean for each section analyzed. Analysis was performed on images captured with a 40× objective. (C) OD of MAP2 stain in E11–12 tissue. (D) OD of E14–15 EphA4 immunolabeling. Filled circles (●) represent dorsal neuropil; open squares (□) represent ventral neuropil.

been established to bind specifically to their target proteins (Soans et al., 1994; Cramer et al., 2002).

We describe our results in the context of the tonotopic organization of NL where best frequencies extend from the rostromedial end of NL (high) to the caudolateral end (low). Throughout the text, high frequency (HF) and low frequency (LF) will be used interchangeably with rostromedial and caudolateral, respectively.

In this study, we wished to determine whether there is a gradient of antigenicity for EphA4 or ephrin-B2 along the tonotopic axis of NL during synaptogenesis. However, it is well known that NL dendrites vary in size and complexity as a function of tonotopic position (Smith and Rubel, 1979; Smith, 1981). Thus, tonotopic gradients of Eph or ephrin labeling density in a region of neuropil could be influenced both by dendritic density as well as protein expression levels. To address this possibility, we first characterized the density of NL neuropil along the axis of tonotopy by staining for the microtubule associated protein MAP2, which labels dendrites. Figure 1 shows the MAP2 staining pattern seen at E12 [Fig. 1(A)] and at E15 [Fig. 1(B)]. MAP2 immunolabeling was largely restricted to the neuropil of NL at both ages tested. At E11–12, staining appears more robust at the low frequency end of the nucleus, decreasing monotonically toward the high frequency end. Figure 1(B) illustrates MAP2 immunostaining at E15. At this age, staining for MAP2 density appears nearly equivalent in neuropil across the nucleus ($n = 3$).

The distribution of immunolabeling was quantified by measuring optical density. These measurements indicate the intensity of immunolabeling averaged within a specified region; they do not provide any indication of the extent of labeling within the nucleus. OD measurements were normalized to the mean OD of staining for MAP2 in the dorsal and ventral regions of NL and are plotted for a representative animal in Figure 1(C) and (D). Each point represents normalized OD of a compartment of neuropil. OD plots for MAP2 increase linearly from the HF end of NL to the LF end in both dorsal (DNP) and ventral neuropil

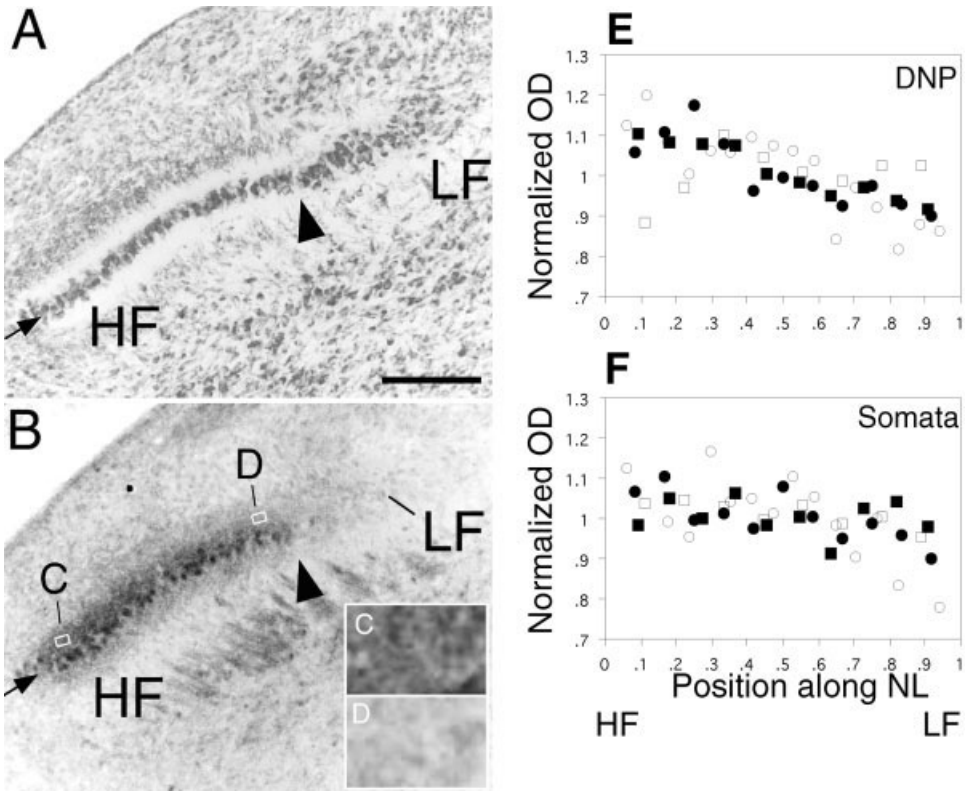

Figure 2 EphA4 immunolabeling in nucleus laminaris (NL) at E11. (A) Parasagittal section from an E11 embryo stained for Nissl showing the location of NL (HF, high frequency; LF, low frequency). (B) Section adjacent to that shown in (A), labeled with an antibody specific for EphA4. EphA4 is localized to cell bodies and dorsal neuropil. The arrow in both panels indicates the line of cell bodies in NL. Arrowheads in (A) and (B) indicate the position along NL where EphA4 immunoreactivity drops below detection level. Scale bar, 100 μm. (C,D) Enlarged view of indicated neuropil areas labeled with EphA4 along the tonotopic axis of NL. The gradient in intensity of label is evident. (E,F) Optical density (OD) measurements describing EphA4 immunolabeling along the tonotopic axis of NL at E10–11. (E) OD measurements describing EphA4 immunolabeling in dorsal neuropil (DNP) of NL at E10–11. Each point indicates OD normalized to the mean of a compartment along the DNP. $R^2 = 0.522$, $p < 0.001$. (F) OD measurements describing immunolabeling in NL somata at E10–11. $R^2 = 0.358$, $p < 0.0001$. Filled circles (●), open circles (○), and open squares (□) represent different animals. OD is normalized to the mean (see Materials and Methods).

(VNP) at E11–12 [Fig. 1(C)]. These data indicate that dendritic density is greater at the low frequency end of the nucleus at E12 (DNP: $R^2 = 0.79$, $p < 0.001$; VNP: $R^2 = 0.769$, $p < 0.001$, $n = 1$). By E15 [Fig. 1(D)], neuropil density gradient is less steep along the axis of tonotopy (DNP: $R^2 = 0.203$, $p < 0.05$; VNP: $R^2 = 0.203$, $p < 0.03$, $n = 1$). These data allowed us to interpret apparent gradients of Eph and ephrin immunolabeling in NL neuropil against a baseline of dendritic density. MAP2 staining also was used to define the spatial extent of NL neuropil. At the low frequency end of NL, where dendritic density was greatest, the neuropil extend further from the somata layer as well (Smith and Rubel, 1979; Smith, 1981).

Gradient of EphA4 at E10–11

Eph receptor tyrosine kinase (RTK) and ephrin immunoreactivity in NL has been described in detail for several developmental time points previously (Cramer et al., 2000; Cramer et al., 2002). The general staining patterns seen here corroborate previous reports. The micrographs presented here, however, show the Eph RTK staining patterns along the tonotopic axis of NL rather than in the coronal plane of section used previously. Figure 2 shows representative examples of NL sectioned along the tonotopic axis and stained for Nissl [Fig. 2(A)] or EphA4 receptor [Fig. 2(B)] at E10–11. As described previously, EphA4 is ex-

pressed in somata and dorsal neuropil of NL at E10–11 [Fig. 2(B)].

At E10–11, EphA4 is expressed in dorsal neuropil in a gradient. Immunolabeling is most intense at the high frequency end of the nucleus and decreases toward the low frequency end [Figs. 2(C,D)]. This gradient was quantified along the length of NL for EphA4 in four animals. OD measurements are shown in Figure 2(E). Each point represents OD measurements for a compartment drawn in the dorsal neuropil; symbols distinguish each animal. Linear regressions calculated for pooled data reveal that, at E10–11, OD consistently decreases monotonically from high frequency to low frequency ends of NL in dorsal neuropil ($R^2 = 0.522$; $p < 0.001$, $n = 4$). This gradient runs counter to the gradient in dendritic density seen with MAP2. Thus, we are confident that the change in OD seen with EphA4 reflects a change in intensity of protein expression along the length of the nucleus. We also calculated the percent change in intensity of staining from the HF quarter to the LF quarter of the nucleus. On average, optical density of dorsal neuropil decreases 13.5% with EphA4 immunolabeling from HF to LF end of NL.

OD measurements for EphA4 expression in NL somata at E10–11 also reveal a mean decrease in immunolabeling of 12.9% between the HF quarter and the LF quarter of the nucleus [Fig. 2(F)]. The overall decrease is fit well with a linear regression ($R^2 = 0.358$; $p < 0.001$).

These measurements were made on the section of NL containing the longest extent of the tonotopic axis. To validate these measurements, we also measured OD for all immunolabeled sections through these brainstems. We measured OD for ten regions that spanned the tonotopic axis of NL. We combined normalized OD measurements for a single brain from the high frequency 30% of the nucleus and from the low frequency 30% of the nucleus to obtain a single value for high and low frequency regions for each brain. The mean normalized OD for the high frequency 30% in the dorsal neuropil was 1.06 ± 0.17 (S.E.M., $n = 4$), while the normalized OD for the low frequency 30% in these brainstems was 0.88 ± 0.035. These were significantly different ($p < 0.02$; paired t test). These results suggest that measurements obtained using the longest section through NL is representative of trends throughout the nucleus.

Absence of EphA4 Immunolabeling at the LF End of the Nucleus

EphA4 antigenicity is not present in somata or neuropil at the caudolateral end of NL at E10–11 [Fig. 2(A), arrowhead]. The point along NL at which EphA4 expression dropped to background levels was coincident with a divergence in the monolayer arrangement of NL as seen in alternate Nissl sections. [For example, compare arrowheads in Figs. 2(A) and (B).] Because OD measurements were made only on immunolabeling that reached a threshold level, this LF region beyond the arrowheads is not included in the quantified assessments of staining presented above. Thus, while the measured gradient along the tonotopic axis is modest, our quantification of the EphA4 immunolabeling gradient is conservative.

EphA4 is expressed more intensely in the dorsal neuropil than in the ventral neuropil at E9–11 (Cramer et al., 2000), but at E12–13, EphA4 is upregulated in ventral neuropil. We analyzed the low levels of EphA4 expression in ventral neuropil at E10–11 and found expression levels had a limited, but significant, correlation with position along the length of the nucleus (data not shown; $R^2 = 0.186$; $p < 0.002$).

We also analyzed EphA4 immunolabeling at a later stage in embryonic development. Figure 3 illustrates immunolabeling for EphA4 in tissue harvested from an embryo at E14. A Nissl section is shown in Figure 3(A) to highlight the extent of NL. At E14–15, EphA4 expression appears most robust at middle frequencies [Fig. 3(B)]. Quantification of the staining shows that immunolabeling remains high along most of the length of NL and drops off slightly at the ends of the nucleus; this pattern is consistent between somata [Fig. 3(C)], dorsal neuropil [DNP; Fig. 3(D)], and ventral neuropil [VNP; Fig. 3(E)].

Steep Gradients in Ligand Expression in Somata and Surrounding Glial Region

At E10–11, the observed gradient in EphA4 immunolabeling is consistent with a role for EphA4 in establishing a tonotopic arrangement of synaptic connections. We next examined whether expression of the Eph ligands, the ephrins, varies along the tonotopic axis of NL at this age. Ephrin-B2, a ligand with high affinity for EphA4, is expressed in NM axons and NL cell bodies at this age (Cramer et al., 2002). We confirmed expression of Ephrin-B2 in NL somata and NM axons [Fig. 4(A–C)] and also observed expression in the tissue outside of the NL neuropil [Fig. 4(A)].

We compared OD between the HF quarter and 70% of the LF end on the nucleus for tissue immunolabeled for ephrin-B2 to estimate the slope of the staining pattern between these regions. We performed this analysis because we observed a distinct staining

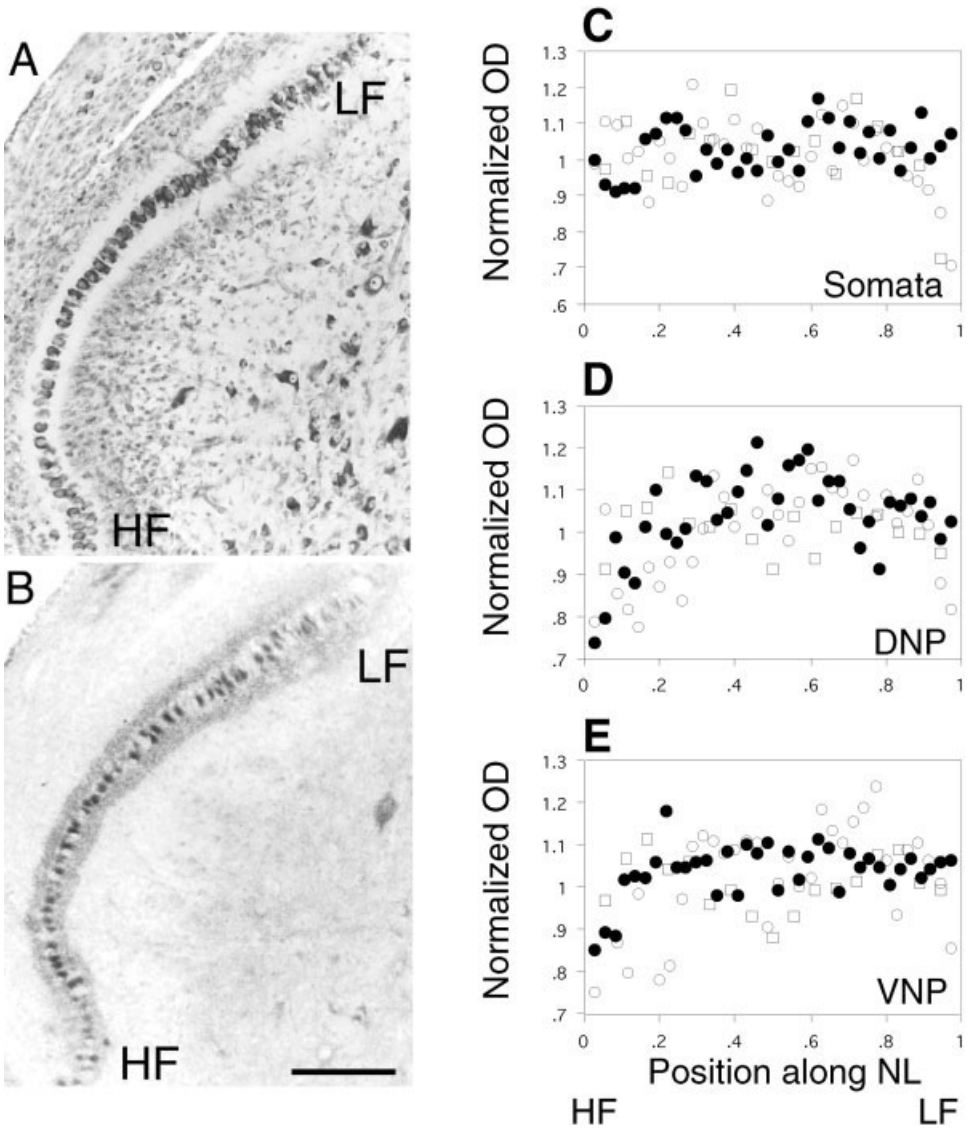

Figure 3 EphA4 immunolabeling in nucleus laminaris (NL) at E14–15. (A) E14 tissue in the parasagittal plane stained for Nissl (HF, high frequency; LF, low frequency). (B) E14 tissue from a section adjacent to that shown in (A) immunolabeled for EphA4. There EphA4 immunolabeling appears intense in somata, dorsal neuropil (DNP), and ventral neuropil (VNP). Scale bar, 100 μm. (C–E) Optical density (OD) measurements for DNP, somata, and VNP at E14–15 representing intensity of EphA4 immunolabeling. (C) Immunolabeling in NL somata is quantified. (D) OD in dorsal neuropil, and (E) ventral neuropil. In all graphs, the position along NL is represented on the abscissa from high to low frequencies. Filled circles (●), open circles (○), and open squares (□) represent different animals. OD is normalized to the mean (see Materials and Methods).

pattern for ephrin-B2 that consistently declined to a minimum relative value at 70% of the LF end.

Our results show that there is a gradient in the expression of ephrin-B2 in somata along 70% of NL's tonotopic axis, decreasing monotonically from the HF end. We observed that ephrin-B2 immunolabeling decreases from the HF end to approximately 70% of the length of the nucleus where it begins to increase to the LF extent of NL. This gradient is robust and includes a mean decrease in OD of 22% (between the HF end and the region of somata 70% of the LF end) [Fig. 4(A)]. Figure 4(D–F) shows OD measurements for ephrin-B2 immunolabeling. Analysis of OD measurements reveals that the gradient in ephrin-B2 expression in this region is highly linear ($r = -0.876$, $R^2 = 0.767$, $p < 0.001$, $n = 4$) [Fig. 4(D)]. The

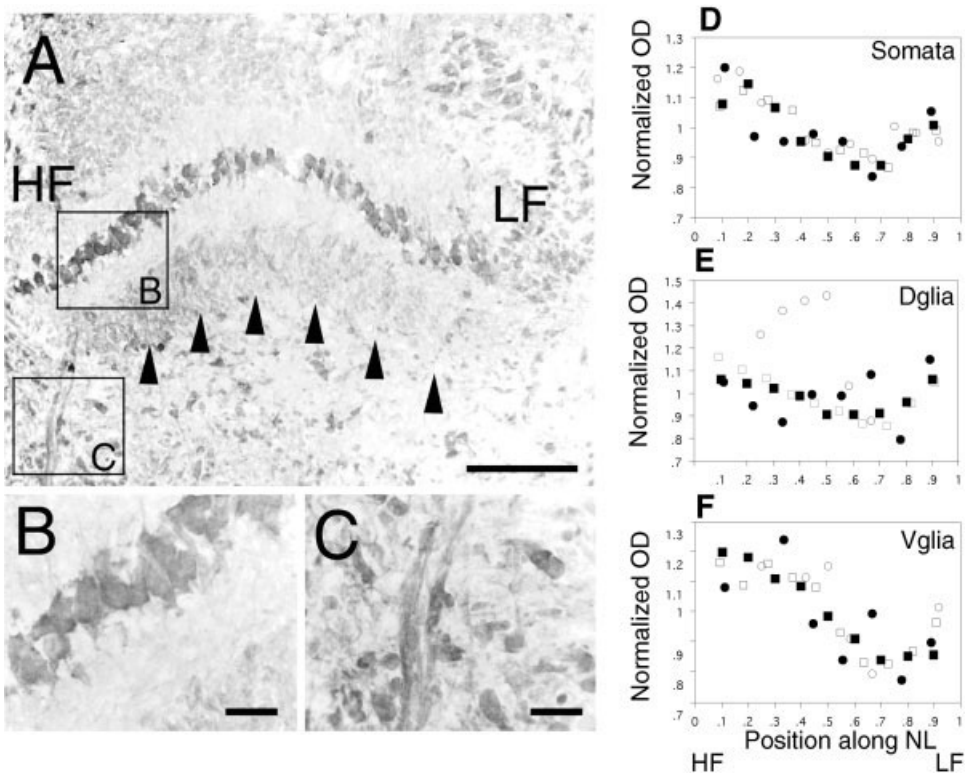

Figure 4 Ephrin-B2 immunolabeling along the length of nucleus laminaris (NL) at E11. (A) Ephrin-B2 is expressed in cell bodies of NL and in high frequency (HF) and low frequency (LF) regions of the nucleus. Expression is more intense in the HF region. Label is also observed in axons innervating NL cells and in the cells outside the neuropil zone of NL (arrowheads), which contains glial cells. The ventral glial region has a tonotopic decrease in Ephrin-B2 immunolabeling intensity. Scale bar, 100 μm. (B) High magnification of image outlined in (A) highlighting the cell bodies of NL with the most pronounced immunolabeling. Scale bar, 20 μm. (C) High magnification of image outlined in (A) highlighting the labeled axons that emerge from nucleus magnocellularis (NM) and innervate NL cells. Scale bar, 20 μm. (D–F) Intensity of ephrin-B2 immunolabeling was quantified by calculating optical density (OD). Graphs plot normalized OD for somata, dorsal glia (Dglia), and ventral glia (Vglia). Symbols represent different animals. (D) Densitometry measurements describing ephrin-B2 immunolabeling in somata along the entire length of NL. The HF 70% contains a strong monotonic decrease described by a linear regression model. $R^2 = 0.767$, $p < 0.0001$. (E) Normalized OD for ephrin-B2 expression levels in the Dglia region. No consistent trend was seen in these measurements. $R^2 = 0.14$, $p < 0.017$. (F) Normalized OD measurements for the Vglia region show a strong trend of decreasing ephrin-B2 immunolabeling in areas immediately ventral to the neuropil layer NL. $R^2 = 0.491$, $p < 0.0001$.

change in OD between the HF end and the LF 30% was significant ($p < 0.0006$, Student's paired t test). The increase in ephrin-B2 immunoreactivity at the extreme LF extent of NL was observed consistently as well.

Ephrin-B2 immunolabeling was observed in the regions immediately adjacent to cell body free zones of the NL neuropil. Previous studies have shown that this area is largely composed of glial cells (Smith and Rubel, 1979; Rubel et al., 1981). Ephrin-B2 expression does not vary consistently with position in the glial region surrounding NL dorsally. OD measurements for the dorsal glial region stained for ephrin-B2 are presented in Figure 4(E) (Dglia). While there was a mean decrease of 20% along the length of the nucleus, the regression model did not fit well ($R^2 = 0.14$).

Ephrin-B2 in the ventral margin immediately surrounding NL neuropil was expressed in a significant gradient [Fig. 4(A), arrowheads]. High-power micrographs reveal that regions juxtaposing NL neuropil express ephrin-B2 [Fig. 4(C)]. The label in these regions was quantified and the results are shown in Figure 4(F). In the ventral glial region (Vglia), eph-

rin-B2 expression is most intense at the rostromedial extent of the section, near the HF end of NL. Ephrin-B2 immunolabeling decreases monotonically toward the caudolateral extent of the section, near the LF end of NL. This gradient is described well with a linear regression model ($R^2 = 0.491$; $p < 0.001$). In the ventral glial region, mean intensity of immunolabeling drops 30% along the length of the nucleus. This change in OD between the HF quarter and LF quarter of NL is significant ($p < 0.01$, paired t test).

In addition to NL somata and surrounding glial regions, ephrin-B2 immunolabeling is present in axons arriving from contralateral NM [Fig. 4(A,C)], as reported previously for E10–11 animals (Cramer et al., 2002). We did not attempt to quantify axonal expression because of the paucity of fibers captured in this plane of section.

DISCUSSION

The main findings in this study are that EphA4 and ephrin-B2 are expressed in gradients along the tonotopic axis of NL during the period of innervation by NM axons. EphA4 expression appears most robust at the high frequency end of the nucleus in the dorsal neuropil, decreasing toward the low frequency end. We have also shown that ephrin-B2 is expressed in a gradient in NL somata along the axis of tonotopy. In addition, ephrin-B2 is expressed in tissue surrounding NL neuropil and, in the ventral glial margin, there is a distinct monotonic gradient. Because of the strong evidence linking gradients of Eph expression to the establishment of topographically precise projections in other systems, our results suggest a potential role for EphA4 and ephrin-B2 in the formation of tonotopically precise connectivity in NL.

A limitation of our quantitative observations is that these measurements cannot be converted to absolute levels of protein and we cannot claim a ratio or interval relationship (e.g., linear, logarithmic, etc.) between variations in our OD measurements and protein levels. It is reasonable to assume an ordinal relationship. That is, our OD measurements indicate relative levels of protein, which may be sufficient to ascertain whether significant differences in expression are present at different ends of the tonotopic axis. In support of this idea, previous studies have shown that the outcome of Eph and ephrin interactions may involve relative and not absolute levels of protein (Brown et al., 2000).

Our results are significant in the context of previously described patterns of Eph family protein expression in the developing auditory brainstem. A striking pattern of EphA4 expression arises at E10–11; EphA4 expression is dramatically greater in dorsal neuropil compared to ventral neuropil (Cramer et al., 2000). EphA4 is then upregulated in ventral neuropil around E12 to become symmetrical in the dorsal and ventral neuropil areas of NL. Conversely, TrkB, a neurotrophin receptor, is expressed predominantly in the ventral neuropil at E10, and this asymmetric expression pattern is maintained through hatching (Cochran et al., 1999; Cramer et al., 2000). Trk receptors and ephrin-B ligands have been shown to share at least one downstream target, the ankyrin repeat-rich membrane spanning (ARMS) protein (Kong et al., 2001).

In addition to EphA4, we have recently reported expression patterns of other Eph receptors and ephrin ligands in the chick auditory brainstem (Cramer et al., 2002). The present study adds an additional degree of detail to the description of expression patterns of Eph molecules in NL. We sectioned brainstems 30° to the parasagittal plane in order to examine expression along the tonotopic axis of NL. We cannot be certain that we have included the entire length of the axis. Mapping studies show that this is the tonotopic axis in embryonic and post-hatch chicks (Rubel and Parks, 1975; Lippe and Rubel, 1985), and we did observe a gradient in dendritic arbor size, suggesting that we have included a substantial portion of the axis of tonotopy (Smith, 1981). An advantage of our approach is that immunolabeling was compared within a single section, rather than between sections. Images of different sections can be captured under slightly different luminance conditions, and efficacy of immunohistochemical reactions may vary between sections; comparing OD in a single section should minimize these potential artifacts from influencing our measurements. We verified that differences in expression levels between high frequency and low frequency regions of NL were present when sections throughout NL were included in the analysis. On the basis of these measurements, it is reasonable to hypothesize that the gradients we observe are involved with the development of topographic projections or nuclear morphology that change as a function of position along the tonotopic axis (Rubel and Parks, 1988).

Ephs in Guiding Tonotopic Development

There is an extensive literature on the role of Eph gradients in establishing topographic maps. In general, Eph gradients involved with topographic map formation in the visual system include countergradients of receptors and ligands (Braisted et al., 1997; Connor et al., 1998; Feldheim et al., 1998; Frisén et al., 1998; Holash et al., 1997; Holmberg et al., 2000;

Walkenhorst et al., 2000). For example, in chick, EphA3 is expressed on retinal ganglion cell axons in a gradient counter to the gradients of ephrin-A5 and ephrin-A2 in the optic tectum (Connor et al., 1998).

In the present report, we show that EphA4 is expressed in a gradient along the tonotopic axis of NL. Ephrin-B2 protein expression in NM axons does not appear to be regulated in a countergradient to EphA4 receptors in NL neuropil. Thus, our data are not clearly analogous to the canonical mechanisms of Eph gradients in establishing topography elsewhere in the nervous system. A further complication to interpreting these results stems from work indicating that protein splice variants and post-translational modifications influence whether an interaction between an Eph receptor and its ligand will result in an adhesive or repulsive contact (Holmberg et al., 2000; Klein, 2001; Mann et al., 2002; Hindges et al., 2002). We did not ascertain whether Eph RTKs or ephrins expressed here were phosphorylated, which can affect their activity. The identification of expression patterns of Eph family proteins in this system does not indicate a functional role, but will nonetheless aid in the design of experiments to test the function of these proteins in the establishment of precise tonotopic connectivity.

Other Potential Roles for Eph RTK and Ephrin Gradients

It is critical to note that dorsal and ventral neuropil receive segregated inputs from ipsilateral and contralateral NM, respectively. Because EphA4 expression is concentrated in the dorsal neuropil at the time these inputs are becoming established (Jackson et al., 1982; Young and Rubel, 1986), it is possible that synaptogenesis and establishment of topography of dorsal and ventral NL involve distinct molecular cues. NM axons are established in the dorsal neuropil around E8, but the development of mature topography occurs primarily between E9 and E13 (Young and Rubel, 1986), during which time EphA4 expression along the tonotopic axis is modified dramatically. It has been shown that the ipsilateral NM axons are topographically organized at the onset of innervation of NL (Young and Rubel, 1986). Conversely, contralateral axons from NM to NL are apposed to the ventral neuropil of NL by E7, but when innervation begins, contralateral axons may be positioned accurately with respect to tonotopy. Tonotopic specificity of contralateral inputs of NL appears to become more precise at around E13 (Young and Rubel, 1986), concurrent with the onset of expression of EphA4 in the ventral neuropil (Cramer et al., 2000).

In addition to EphA4 expression, both dorsal and ventral neuropil express EphB2 (Cramer et al., 2002). Both EphA4 and EphB2 may influence axons through reverse signaling (Holland et al., 1996; Brückner et al., 1997). Several groups have shown that EphB2 is involved in synaptogenesis, thus the contact between axons expressing ephrin-B2 and EphB2 may be facilitory for adhesion (Dalva et al., 2000; Grunwald et al., 2001).

The possible function of Eph gradients in NL is not restricted to map formation. Several phenomena have been reported to progress along the tonotopic axis of NL including dendritic pruning, dendritic growth, and cell death (Smith, 1981; Rubel et al., 1976). Eph gradients may be involved with signaling in these events. A well-characterized feature of NL dendrites is their gradient in size along the tonotopic axis (Smith and Rubel, 1979). This gradient appears to first form at E10 (Smith, 1981). A plausible role for Eph gradients in NL at E10–11 would be to play a part in regulating this gradient in dendritic arbor size. The spatiotemporal expression patterns of Eph family proteins in NL and surrounding regions thus suggests several possible roles for these proteins in the maturation of the auditory brainstem.

We thank Dale Cunningham for assistance with histochemical procedures, and Glen MacDonald for help with densitometry software. Special thanks to Dr. David J. Perkel for his gracious support during the preparation of the manuscript.

REFERENCES

Braisted JE, McLaughlin T, Want HU, Friedman GC, Anderson DJ, O'Leary DDM. 1997. Graded and lamina-specific distributions of ligands of EphB receptor tyrosine kinases in the developing retinotectal system. Dev Biol 191:14–28.

Brown A, Yates PA, Burrola P, Ortuño D, Vaidya A, Jessell TM, Pfaff SL, O'Leary DDM, Lemke G. 2000. Topographic mapping from the retina to the midbrain is controlled by relative but not absolute levels of EphA receptor signaling. Cell 102:77–88.

Brückner K, Pasquale EB, Klein R. 1997. Tyrosine phosphorylation of transmembrane ligands for Eph receptors. Science 275:1640–1643.

Carr CE, Konishi M. 1990. A circuit for detection of interaural time differences in the brain stem of the barn owl. J Neurosci 10:3227–3246.

Cheng HJ, Nakamoto M, Bergemann AD, Flanagan JG. 1995. Complementary gradients in expression and binding of ELF-1 and Mck4 in development of the topographic retinotectal projection map. Cell 82:371–381.

Cline HT, Debski EA, Constantine-Paton M. 1987. N-meth-

yl-D-aspartate receptor antagonist desegregates eye-specific stripes. Proc Natl Acad Sci USA 84:4342–4345.

Cochran SL, Stone JS, Bermingham-McDonogh O, Akers SR, Lefcort F, Rubel EW. 1999. Ontogenetic expression of Trk neurotrophin receptors in the chick auditory system. J Comp Neurol 413:271–288.

Connor RJ, Menzel P, Pasquale EB. 1998. Expression and tyrosine phosphorylation of Eph receptors suggest multiple mechanisms in patterning of the visual system. Dev Biol 193:21–35.

Cramer KS, Rosenberger MH, Frost DM, Cochran SL, Pasquale EB, Rubel EW. 2000. Developmental regulation of EphA4 expression in the chick auditory brainstem. J Comp Neurol 246:270–278.

Cramer KS, Karam SD, Bothwell M, Cerretti DP, Pasquale EB, Rubel EW. 2002. Expression of EphB receptors and EphrinB ligands in the developing chick auditory brainstem. J Comp Neurol 452:51–64.

Dalva MB, Takasu MA, Lin MZ, Shamah SM, Hu L, Gale NW, Greenberg ME. 2000. EphB receptors interact with NMDA receptors and regulate excitatory synapse formation. Cell 103:945–956.

Dearborn R Jr, He Q, Kunes S, Dai Y. 2002. Eph receptor tyrosine kinase-mediated formation of a topographic map in the Drosophila visual system. J Neurosci 22:1338–1349.

Drescher U, Kremoser C, Handwerker C, Loschinger J, Noda M, Bonhoeffer F. 1995. In vitro guidance of retinal ganglion cell axons by RAGS, a 25 kDa tectal protein related to ligands for Eph receptor tyrosine kinases. Cell 82:359–370.

Eph Nomenclature Committee. 1997. Unified nomenclature for Eph family receptors and their ligands, the ephrins. Cell 90:403–404.

Feldheim DA, Vanderhaeghen P, Hansen MJ, Frisén J, Lu Q, Barbacid M, Flanagan JG. 1998. Topographic guidance labels in a sensory projection to the forebrain. Neuron 21:1303–1313.

Frisén J, Yates PA, McLaughlin T, Friedman GC, O'Leary DDM, Barbacid M. 1998. Ephrin-A5 (AL-1/RAGS) is essential for proper retinal axon guidance and topographic mapping in the mammalian visual system. Neuron 20:235–243.

Gao PP, Zhang JH, Yokoyama M, Racey B, Dreyfus CF, Black IB, Zhou R. 1996. Regulation of topographic projection in the brain: Elf-1 in the hippocamposeptal system. Proc Natl Acad Sci USA 93:11161–11166.

Grunwald IC, Korte M, Wolfer D, Wilkinson GA, Unsicker K, Lipp HP, Bonhoeffer T, Klein R. 2001. Kinase-independent requirement of EphB2 receptors in hippocampal synaptic plasticity. Neuron 32:1027–1040.

Hamburger V, Hamilton H. 1951. A series of normal stages in the development of the chick embryo. J Morphol 88:49–92.

Hindges R, McLaughlin T, Genoud N, Henkemeyer M, O'Leary DDM. 2002. EphB forward signaling controls directional branch extension and arborization required for dorsal-ventral retinotopic mapping. Neuron 35:475–487.

Holash JA, Soans C, Chong LD, Shao H, Dixit VM, Pasquale EB. 1997. Reciprocal expression of the Eph receptor Cek5 and its ligand(s) in the early retina. Dev Biol 182:256–269.

Holland SJ, Gale NW, Mbamalu G, Yancopoulos GD, Henkemeyer M, Pawson T. 1996. Bidirectional signalling through the EPH-family receptor Nuk and its transmembrane ligands. Nature 383:722–725.

Holmberg J, Clarke DL, Frisén J. 2000. Regulation of repulsion versus adhesion by different splice forms of an Eph receptor. Nature 408:203–206.

Jackson H, Hackett JT, Rubel EW. 1982. Organization and development of brain stem auditory nuclei in the chick: ontogeny of postsynaptic responses. J Comp Neurol 210:80–86.

Klein R. 2001. Excitatory Eph receptors and adhesive ephrin ligands. Curr Opin Cell Biol 13:196–203.

Kong H, Boulter J, Weber JL, Lai C, Chao MV. 2001. An evolutionarily conserved transmembrane protein that is a novel downstream target of neurotrophin and ephrin receptors. J Neurosci 21:176–185.

Leake PA, Snyder RL, Hradek GT. 2002. Postnatal refinement of auditory nerve projections to the cochlear nucleus in cats. J Comp Neurol 448:6–27.

Lippe W, Rubel EW. 1985. Ontogeny of tonotopic organization of brain stem auditory nuclei in the chicken: implications for development of the place principle. J Comp Neurol 237:273–289.

Mann F, Ray S, Harris W, Holt C. 2002. Topographic mapping in dorsoventral axis of the Xenopus retinotectal system depends on signaling through ephrin-B ligands. Neuron 35:461–473.

Parks TN, Rubel EW. 1975. Organization and development of brain stem auditory nuclei of the chicken: organization of projections from N. magnocellularis to N. laminaris. J Comp Neurol 164:435–448.

Rubel EW, Cramer KS. 2002. Choosing axonal real estate: location, location, location. J Comp Neurol 448:1–5.

Rubel E, Parks T. 1988. Organization and development of the avian brain-stem auditory system. In Edelman GM, Gall WE, and Cowan WM (Eds.). Auditory Function: Neurobiological bases of hearing. New York: John Wiley & Sons. pp 3–92.

Rubel EW, Parks TN. 1975. Organization and development of brain stem auditory nuclei of the chicken: tonotopic organization of N. magnocellularis and N. laminaris. J Comp Neurol 164:411–434.

Rubel EW, Smith DJ, Miller LC. 1976. Organization and development of brain stem auditory nuclei of the chicken: ontogeny of N. magnocellularis and N. laminaris. J Comp Neurol 166:469–490.

Rubel EW, Smith ZDJ, Steward O. 1981. Sprouting in the avian brainstem auditory pathway: dependence on dendritic integrity. J Comp Neurol 202:397–414.

Smith DJ, Rubel EW. 1979. Organization and development of

brain stem auditory nuclei of the chicken: dendritic gradients in nucleus laminaris. J Comp Neurol 186:213–240.

Smith ZDJ. 1981. Organization and development of brain stem auditory nuclei of the chicken: dendritic development in N. laminaris. J Comp Neurol 203:309–333.

Soans C, Holash JA, Pasquale EB. 1994. Characterization of the expression of the Cek8 receptor-type tyrosine kinase during development and in tumor cell lines. Oncogene 9:3353–3361.

Walkenhorst J, Dütting D, Handwerker C, Huai J, Tanaka H, Drescher U. 2000. The EphA4 receptor tyrosine kinase is necessary for the guidance of nasal retinal ganglion cell axons in vitro. Mol Cell Neurosci 16:365–375.

Young SR, Rubel EW. 1983. Frequency-specific projections of individual neurons in chick brainstem auditory nuclei. J Neurosci 3:1373–1378.

Young SR, Rubel EW. 1986. Embryogenesis of arborization pattern and topography of individual axons in N. laminaris of the chicken brain stem. J Comp Neurol 254:425–459.